Peer reviewed version

Link to published version (if available):
10.1109/WCNC.2009.4917731

Link to publication record in Explore Bristol Research
PDF-document

Frequency-Domain Transmit Processing for MIMO SC-FDMA in Wideband Propagation Channels

Mohamed Noune and Andrew Nix

Centre for Communications Research, University of Bristol
Merchants Ventures Building, Woodland Road, BS8 1TJ, Bristol UK
Email: {Mohamed.Noune,Andy.Nix}@bristol.ac.uk

Abstract— Recently there has been considerable interest in the use of Single Carrier Frequency Division Multiple Access (SC-FDMA) as the uplink transmission scheme for the 3GPP Long Term Evolution (LTE) standard. This paper investigates different Multiple Input Multiple-Output (MIMO) techniques for uplink SC-FDMA. Here we demonstrate how the transmitter can exploit the available channel information, through precoding and pre-equalization, in order to combat the frequency selective nature of the propagation channel and improve the system's performance under fading. In this work we investigate the achievable system capacity, and the Peak-to-Average Power Ratio (PAPR) characteristics of the precoded and pre-equalized SC-FDMA waveform. We consider unitary precoding for MIMO, as well as pre-equalization for a Multiple-Input Single-Output (MISO) system with Maximum Ratio Combining (MRC), Equal Gain Combining (EGC), Zero Forcing (ZF), and Minimum Mean Square Error (MMSE) algorithms. Results reported in this paper show that ZF pre-equalization for SISO SC-FDMA is capable of achieving the Shannon Capacity limit for faded channels, with a BER performance that is identical to an AWGN channel, and that pre-equalized increases the capacity of MIMO SC-FDMA systems.

Keywords: 3GPP LTE, MIMO, SC-FDMA, Frequency-Domain Pre-equalization, PAPR, Equalization, Beamforming.

I. INTRODUCTION

THE significant expansion seen in mobile and cellular technology over the last two decades is a direct result of the increasing demand for high data rate transmissions over bandwidth and power limited wireless channels. This requirement for high data rates results in significant inter-symbol interference (ISI) for single carrier systems, and thereby requires the use of robust coding and powerful signal processing techniques in order to overcome the time and frequency selective natures of the propagation channel. Recent examples include different transmitter/receiver optimization techniques for high data rate transmissions as well as the use of multiple antennas at both the transmitter and receiver, known as Multiple-Input Multiple-Output (MIMO). MIMO takes advantage of the spatial separation between antenna elements to create uncorrelated spatial channels, and to exploit higher levels of spatial diversity. This translates to improved spectral and power efficiency. These techniques are particularly attractive at the base station, where large antenna spacing are more easily accommodated.

The Third Generation Partnership Project (3GPP) Long Term Evolution (LTE) radio access standard is based on shared channel access providing peak data rates of 75 Mbps in the uplink and 300 Mbps in the downlink and supports different carrier bandwidths (1.25–20 MHz) in both Frequency Division Duplex (FDD) and Time Division Duplex (TDD) modes [1]. A working assumption in the LTE standard is the use of Orthogonal Frequency Division Multiple Access (OFDMA).

OFDMA is an OFDM-based multiple access scheme [2] that provides each user with a unique fraction of the system bandwidth. OFDMA is highly suitable for broadband wireless access networks (particularly the downlink) since it combines scalability, multipath robustness and MIMO compatibility [2]. OFDMA is very sensitive to frequency offset and phase noise, and thus requires accurate frequency and phase synchronization. In addition, OFDMA is characterized by a high PAPR, and for a given peak-power limited amplifier this results in a lower mean transmit level at the handset. For these reasons, OFDMA is not well-suited to the uplink transmission. SC-FDMA, also known as DFT precoded OFDMA [1], has been proposed for uplink cellular applications.

Although the 3GPP standard only adopts MIMO transmission for downlink, MIMO can be used in conjunction with SC-FDMA for uplink transmission. This will improve system capacity and overcome the power limitations of these systems. MIMO can be divided into three main types or categories. Firstly, in precoding, also known as beamforming, the same signal is emitted from each of the transmit antennas with appropriate phase and gain weighting such that the signal power is maximized at the receiver input. This increases the signal gain from constructive combining [5]- [7]. In [11], a study of the PAPR characteristics of beamforming with unitary precoding for SC-FDMA has shown that the increase in PAPR of the precoded waveform is not significant when compared to the single antenna system or the non-precoded MIMO SC-FDMA case. In addition, amplitude clipping can be used in order to maintain the PAPR below a certain level at the expense of a performance degradation. Secondly, Spatial Multiplexing (SM), [6]- [8], aims to increase the capacity of the system for the same bandwidth without any increase in the transmit power. Finally, Transmit Diversity (TD) aims to increase the diversity order of the system. In the context of SC-FDMA, [12] shows the possibility of employing TD for SC-FDMA in the form of Space-Time/Frequency Block Coding (STBC/SFBC), or the more novel Single Carrier Space-Frequency Block Coding (SC-SFBC). In [4], a study of the PAPR characteristics together with the error performance of MIMO SC-FDMA was presented for both SM and TD. As was shown, both the PAPR and error performance are highly influenced by the choice of the sub-carrier mapping and vary from one MIMO scheme to the other. It was also shown that pulse shaping can be used to reduce the high PAPR of MIMO SC-FDMA, resulting in a performance degradation for both SM and TD.

The goal of this article is to demonstrate the link performance of MIMO SC-FDMA when spatial equalization is used at the transmitter. Here, we present a study of the Peak-to-Average Power Ratio (PAPR) characteristics and the achievable system

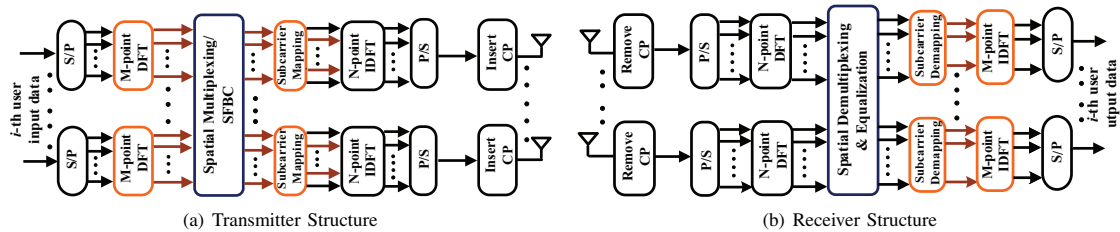(a) Transmitter Structure   (b) Receiver Structure

Fig. 1. Transceiver structure for MIMO SC-FDMA.

capacity of the precoded MIMO and pre-equalized MISO SC-FDMA waveforms. We consider unitary precoding, as well as pre-equalization using a range of diversity combining schemes, namely Maximum Ratio Combining (MRC), Equal Gain Combining (EGC), Zero Forcing (ZF), and the Minimum Mean Square Error (MMSE) algorithm. This paper is organized as follows. In section II the MIMO SC-FDMA transmission model is given. Sections III and IV provide an overview of the MIMO precoding and Transmit Diversity pre-equalization techniques for MIMO SC-FDMA, respectively. In section V we present the channel capacity for MIMO SC-FDMA with precoding and pre-equalization. Simulation results and conclusions are presented in sections VI and VII respectively.

II. MIMO SC-FDMA Transmission

3GPP LTE [1]- [3] is a driving force in the improvement of mobile communication standards [3]. A working assumption for 3GPP LTE is the use of SC-FDMA on the uplink. The principle of SC-FDMA signaling is presented in [9]- [10]. For high data rate wireless communications, multiuser transmission can be achieved through OFDMA and/or SC-FDMA. Since OFDMA waveforms are characterized by their high dynamic range as a result of the IDFT spread, which translates to a high PAPR, SC-FDMA is favored for the uplink transmission. Fig. 1 shows the structure of the $\mathbf{N}_T$-by-$\mathbf{N}_R$ MIMO SC-FDMA system considered in this paper. For the i-th user, for the j-th transmit antenna, and for each block of M data samples $\mathbf{x}_j^{(i)} = \left[x_{j,0}^{(i)}, x_{j,1}^{(i)}, \cdots, x_{j,M-1}^{(i)}\right]^{\mathcal{T}}$, the transmitter maps the corresponding M frequency components of the block, $\mathbf{X}_j^{(i)} = \left[X_{j,0}^{(i)}, X_{j,1}^{(i)}, \cdots, X_{j,M-1}^{(i)}\right]^{\mathcal{T}}$, resulting from an $M-$point DFT of the data samples, onto a set of M active sub-carriers selected from a total of $N = QM$ sub-carriers ($Q > 1$).

In this paper we consider distributed and localized SC-FDMA (D-FDMA and L-FDMA respectively) [9]. We denote the sub-carrier mapping transform matrix for the i-th user by $\mathbf{D}_i$. The entries of this matrix for both D-FDMA and L-FDMA are given in Equations (1) and (2) respectively:

$$\mathbf{D}_i = \begin{array}{l} \left[\mathbf{0}_{(s_i-1)M \times M}; \quad \left(\mathbf{u}_i^M\right)^{\mathcal{T}}; \mathbf{0}_{Q' \times M}; \left(\mathbf{u}_{i+Q'}^M\right)^{\mathcal{T}}; \right. \\ \left. \cdots ; \mathbf{u}_{i+MQ'}^{\mathcal{T}}; \mathbf{0}_{(Q-Q')M \times M} \right] \end{array} \quad (1)$$

$$\mathbf{D}_i = \left[\mathbf{0}_{(i-1)M \times M}; \mathbf{I}_M; \mathbf{0}_{(Q-i)M \times M}\right] \quad (2)$$

The sub-carrier mapping produces $\widetilde{\mathbf{X}}_j^{(i)} = \mathbf{D}_i \mathbf{X}_j^{(i)}$ such that $\widetilde{\mathbf{X}}_j^{(i)} = \left[\widetilde{X}_{j,0}^{(i)}, \widetilde{X}_{j,1}^{(i)}, \cdots, \widetilde{X}_{j,N-1}^{(i)}\right]^{\mathcal{T}}$. $\widetilde{\mathbf{X}}_j^{(i)}$ is processed by the N-point Inverse DFT (IDFT) to produce the time-domain transmitted signal $\widetilde{\mathbf{x}}_j^{(i)} = \left[\widetilde{x}_{j,0}^{(i)}, \widetilde{x}_{j,1}^{(i)}, \cdots, \widetilde{x}_{j,N-1}^{(i)}\right]^{\mathcal{T}}$.

The SC-FDMA transmitted signal can be represented by:

$$\widetilde{\mathbf{x}}_j^{(i)} = \mathbf{P}\mathbf{F}_N^{-1}\mathbf{D}_i\mathbf{F}_M\mathbf{x}_j^{(i)} \quad (3)$$

where $\mathbf{F}_N^{-1}$ and $\mathbf{F}_M$ are the N-point IDFT and M-point DFT matrix respectively. The generic K-point DFT matrix has entries $[\mathbf{F}_K]_{p,q} = e^{-j2\pi\frac{pq}{K}}$, and its inverse is $\mathbf{F}_K^{-1} = \mathbf{F}_K^{\mathcal{H}}$, where $(\bullet)^{\mathcal{H}}$ denotes the *Hermitian* transpose. $\mathbf{P}$ represents the cyclic prefix (CP) insertion matrix:

$$\mathbf{P} = [\mathbf{C}, \mathbf{I}_N]^{\mathcal{T}}, \quad \mathbf{C} = \left[\mathbf{0}_{P \times (N-P)}, \mathbf{I}_P\right]^{\mathcal{T}}$$

The received SC-FDMA signal on the m-th receive antenna, $r_{m,n}^{(i)}$ at time n, for a multipath fading MIMO channel corrupted by Additive White Gaussian Noise, $w_{m,n}^{(i)}$, with variance N_o is given by:

$$r_{m,n}^{(i)} = \sum_{j=1}^{\mathbf{N}_T}\sum_{l=0}^{L} h_{j,m}^k \widetilde{x}_{j,n-l}^{(i)} + w_{m,n}^{(i)} \quad (4)$$

We denote $\mathbf{R}_k^{(i)}$, $\widetilde{\mathbf{X}}_k^{(i)}$ and $\mathbf{W}_k^{(i)}$ be the k-th sub-carrier of the received signal, the transmitted signal and the noise signal at the receiver front-end, respectively, where: $\mathbf{R}_k^{(i)} = \left[\mathbf{R}_{k,1}^{(i)}, \mathbf{R}_{k,2}^{(i)}, \cdots, \mathbf{R}_{k,\mathbf{N}_T}^{(i)}\right]^{\mathcal{T}}$, $\widetilde{\mathbf{X}}_k^{(i)} = \left[\widetilde{\mathbf{X}}_{k,1}^{(i)}, \widetilde{\mathbf{X}}_{k,2}^{(i)}, \cdots, \widetilde{\mathbf{X}}_{k,\mathbf{N}_T}^{(i)}\right]^{\mathcal{T}}$ and $\mathbf{W}_k^{(i)} = \left[\mathbf{W}_{k,1}^{(i)}, \mathbf{W}_{k,2}^{(i)}, \cdots, \mathbf{W}_{k,\mathbf{N}_T}^{(i)}\right]^{\mathcal{T}}$.

By taking the N-point DFT of both sides in equation (4), the k-th sub-carrier of i-th user's received data is given by:

$$\mathbf{R}_k^{(i)} = \mathbf{H}_k\widetilde{\mathbf{X}}_k^{(i)} + \mathbf{W}_k^{(i)} \quad (5)$$

where $\mathbf{H}_k$ denotes the k-th sub-carrier of the MIMO channel frequency response given by

$$\mathbf{H}_k = \begin{bmatrix} \overline{\mathbf{H}}_{1,1}^k & \overline{\mathbf{H}}_{1,2}^k & \cdots & \overline{\mathbf{H}}_{1,\mathbf{N}_T}^k \\ \overline{\mathbf{H}}_{2,1}^k & \overline{\mathbf{H}}_{2,2}^k & \cdots & \overline{\mathbf{H}}_{2,\mathbf{N}_T}^k \\ \vdots & \ddots & \ddots & \vdots \\ \overline{\mathbf{H}}_{\mathbf{N}_R,1}^k & \overline{\mathbf{H}}_{\mathbf{N}_R,2}^k & \cdots & \overline{\mathbf{H}}_{\mathbf{N}_R,\mathbf{N}_T}^k \end{bmatrix}$$

III. Unitary Precoding for MIMO SC-FDMA

When the channel information is available at the transmitter, via feedback from the receiver or through the reciprocity principle in a duplex system, it is possible to increase the channel capacity by exploiting the spatial sub-channels [6]. This is achieved by distributing the transmit energy across the sub-spatial channel for the frequency flat channels, and across space and frequency for the frequency selective MIMO channel, in order to increase the spectral efficiency. Optimal power allocation is achieved through the waterpouring algorithm, as described in [6]. Transmit eigen-beamforming with unitary precoding exploits the eigen-structure of the channel in order to achieve spatial multiplexing [16].

From the Singular Value Decomposition (SVD) of the MIMO channel matrix $\mathbf{H}_k$, $\mathbf{H}_k = \mathbf{U}_k\mathbf{\Lambda}_k\mathbf{V}_k^{\mathcal{H}}$, it is possible to access the spatial modes of the MIMO channel matrix through the

multiplication of the transmitted signal $\widetilde{\mathbf{X}}_k^{(i)}$ by $\mathbf{V}_k$ prior to transmission and the multiplication of the received signal $\mathbf{R}_k^{(i)}$, by $\mathbf{U}^{\mathcal{H}_k}$ at the receiver. The input-output relationship of this operation is given by:

$$\widetilde{\mathbf{R}}_k^{(i)} = \mathbf{U}_k^{\mathcal{H}} \left(\mathbf{H}_k \mathbf{V}_k \widetilde{\mathbf{X}}_k^{(i)} + \mathbf{W}_k^{(i)} \right) = \mathbf{\Lambda}_k \widetilde{\mathbf{X}}_k^{(i)} + \widetilde{\mathbf{W}}_k^{(i)} \quad (6)$$

This shows that with channel knowledge at the transmitter, $\mathbf{H}_k$ can be decomposed into r parallel SISO channels, where r is the rank of $\mathbf{H}_k$, satisfying:

$$\widetilde{\mathbf{R}}_{j,k}^{(i)} = \sqrt{\lambda_{j,k}} \widetilde{\mathbf{X}}_{j,k}^{(i)} + \widetilde{\mathbf{W}}_{j,k}^{(i)}, \quad j = 1, 2, \cdots, r \quad (7)$$

Given a MIMO system with an average power constraint, the concept of water filling aims to exploit the spatial decomposition of the MIMO channel given channel knowledge at the transmitter, by allocating optimal energy onto each spatial of the modes, which will increase the capacity of each spatial mode. Using the optimal power allocation scheme described in [14], the optimum power, $\gamma_{j,k}$, allocated to the spatial mode j, is given by:

$$\gamma_{j,k} = \begin{cases} \mu_k - \frac{1}{\lambda_{j,k}} & : \mu_k \geq \frac{1}{\lambda_{j,k}} \\ 0 & : \text{otherwise} \end{cases} \quad (8)$$

where μ is the cutoff SNR level below which no eigen-mode transmission is performed. μ is given by:

$$\mu_k = \mathbf{N}_T \left[1 + \frac{N_o}{E_s} \sum_{i=1}^{r} \frac{1}{\lambda_{j,k}} \right] \quad (9)$$

IV. MISO SC-FDMA WITH PRE-EQUALIZATION

The main focus of our investigations in this section is constrained pre-equalization for Multiple-Input Single-Output (MISO) SC-FDMA, where the mean transmit power is constrained to be the same as the standard transmission case. We start by deriving the pre-equalizer weight without any power constraints and then introduce the

A. Unconstrained Pre-equalization

We define $\overline{\mathbf{G}}_{j,k}^{(i)}$ the pre-equalization coefficients without power constraints. The different design criteria considered in this paper are:

1) Maximum Ratio Combining: MRC pre-equalization aims to maximize the instantaneous SNR at the receiver's front end. Under the MRC criterion, the pre-equalization weights are:

$$\overline{\mathbf{G}}_{j,k}^{(i)} = \left(\overline{\mathbf{H}}_{j,k} \right)^* \quad (10)$$

2) Equal Gain Combining: In order for all the sub-carriers to arrive at the receiver in phase, phase equalization can be performed at the transmitter in the form of EGC. Under the EGC criterion, the pre-equalization weights are:

$$\overline{\mathbf{G}}_{j,k}^{(i)} = \frac{\left(\overline{\mathbf{H}}_{j,k} \right)^*}{\left| \overline{\mathbf{H}}_{j,k} \right|} \quad (11)$$

3) Zero-Forcing: The pre-equalizer constructed under the ZF criterion represents the inverse of the channel's frequency response. For the i-th user and the j-th transmit antenna, the ZF pre-equalization weights are therefore:

$$\overline{\mathbf{G}}_{j,k}^{(i)} = \frac{\left(\overline{\mathbf{H}}_{j,k} \right)^*}{\left| \overline{\mathbf{H}}_{j,k} \right|^2} \quad (12)$$

4) Minimum Mean Square Error: The pre-equalization weights under the MMSE frequency-domain pre-equalizer for the j-th transmit antenna satisfy:

$$e^2 = \sum_{k \in \Psi_i} \left| \overline{\mathbf{G}}_{j,k}^{(i)} \overline{\mathbf{H}}_{j,k} - 1 \right|^2 \quad (13)$$

The pre-equalizer weights are therefore given by:

$$\overline{\mathbf{G}}_{j,k}^{(i)} = \frac{\overline{\left(\overline{\mathbf{H}}_{j,k} \right)^*}}{\left| \overline{\mathbf{H}}_{j,k} \right|^2 + \lambda}, \quad (14)$$

λ must be found by numerical computation as it depends on the channel delay profile. If N_o, the variance of the additive noise at the receiver front-end, is known at the transmitter, then λ in equation (15) equals N_o.

$$\overline{\mathbf{G}}_{j,k}^{(i)} = \frac{\left(\overline{\mathbf{H}}_{j,k} \right)^*}{\left| \overline{\mathbf{H}}_{j,k} \right|^2 + N_o} \quad (15)$$

B. Constrained Pre-equalization

For the j-th transmit antenna, the k-th sub-carrier weight of the power constrained frequency-domain pre-equalization filter, $\mathbf{G}_{j,k}^{(i)}$, for the i-th user satisfy:

$$\sum_{k \in \Psi_i} \left| \mathbf{G}_{j,k}^{(i)} \widetilde{\mathbf{X}}_{j,k}^{(i)} \right|^2 = \sum_{k \in \Psi_i} \left| \widetilde{\mathbf{X}}_{j,k}^{(i)} \right|^2 \quad (16)$$

Let $\overline{\mathbf{G}}_{j,k}^{(i)}$ be the k-th sub-carrier pre-equalization coefficient without power constraints. We define $\mathbf{P}_j$ the normalization factor for the j-th transmit antenna, such that $\mathbf{G}_{j,k}^{(i)} = \overline{\mathbf{G}}_{j,k}^{(i)} \mathbf{P}_j$. From equation (16):

$$\frac{1}{M} \sum_{k \in \Psi_i} \left| \mathbf{G}_{j,k}^{(i)} \right|^2 = \frac{1}{M} \sum_{k \in \Psi_i} \left| \overline{\mathbf{G}}_{j,k}^{(i)} \mathbf{P}_j \right|^2 = 1 \quad (17)$$

It follows from equation (17) $\mathbf{P}_j$ is given by:

$$\mathbf{P}_j = \sqrt{M \left(\sum_{k \in \Psi_i} \left| \overline{\mathbf{G}}_{j,k}^{(i)} \right|^2 \right)^{-1}}$$

V. CAPACITY OF MIMO SC-FDMA

The channel capacity of the i-th user, $\mathbf{C}_k^{(i)}$, at the k-th sub-carrier is:

$$\mathbf{C}_k^{(i)} = \log_2 \det \left(\mathbf{I}_{\mathbf{N}_R} + \frac{E_s}{\mathbf{N}_T N_o} \mathbf{H}_k \mathbf{H}_k^{\mathcal{T}} \right) \quad (18)$$

The instantaneous capacity of the i-th user, $\mathbf{C}^{(i)}$, can therefore be given by:

$$\mathbf{C}^{(i)} = \sum_{k \in \Psi_i} \log_2 \det \left(\mathbf{I}_{\mathbf{N}_R} + \frac{E_s}{\mathbf{N}_T N_o} \mathbf{H}_k \mathbf{H}_k^{\mathcal{H}} \right) \quad (19)$$

A. Capacity Under Unitary Precoding

Given the Eigenvalue Decomposition (EVD) of $\mathbf{H}_k \mathbf{H}_k^{\mathcal{H}}$, $\mathbf{H}_k \mathbf{H}_k^{\mathcal{H}} = \mathbf{Q}_k \mathbf{\Lambda} \mathbf{Q}_k^{\mathcal{H}}$, we can re-write equation (19) as:

$$\mathbf{C}^{(i)} = \sum_{k \in \Psi_i} \sum_{j=1}^{r} \log_2 \left(1 + \frac{E_s}{\mathbf{N}_T N_o} \lambda_{j,k} \right) \quad (20)$$

As mentioned previously, optimal power allocation scheme described in [14], the optimum power

$$\mathbf{C}^{(i)} = \sum_{k \in \Psi_i} \sum_{j=1}^{r} \log_2 \left(1 + \frac{E_s}{\mathbf{N}_T N_o} \gamma_{j,k} \lambda_{j,k} \right) \quad (21)$$

B. Capacity of Pre-equalized MISO Systems

For MISO transmission, as a result of pre-equalization, the k-th sub-carrier of the received signal for the i-th user can be expressed as:

$$\mathbf{R}_k^{(i)} = \widetilde{\mathbf{H}}_k^{\mathcal{H}} \widetilde{\mathbf{X}}_k^{(i)} + \mathbf{W}_k^{(i)} \tag{22}$$

where $\widetilde{\mathbf{H}}_k$ is the equivalent channel's frequency response as a result of pre-equalization at the k-th sub-carrier: where

$$\widetilde{\mathbf{H}}_k = \left[\begin{array}{cccc} H_{1,k}G_{1,k}^{(i)}, & H_{2,k}G_{2,k}^{(i)}, & \cdots, & H_{\mathbf{N}_T,k}G_{\mathbf{N}_T,k}^{(i)} \end{array} \right]^T$$

The instantaneous capacity of the i-th user, $\mathbf{C}^{(i)}$, can therefore be given by:

$$
\begin{aligned}
\mathbf{C}^{(i)} &= \sum_{k \in \Psi_i} \log_2 \left(1 + \frac{E_s}{\mathbf{N}_T N_o} \widetilde{\mathbf{H}}_k^{\mathcal{H}} \widetilde{\mathbf{H}}_k \right) \\
&= \sum_{k \in \Psi_i} \log_2 \left(1 + \frac{E_s}{\mathbf{N}_T N_o} \sum_{j=1}^{\mathbf{N}_T} \left| \mathbf{P}_j \mathbf{H}_{j,k} \overline{\mathbf{G}}_{j,k}^{(i)} \right|^2 \right)
\end{aligned} \tag{23}
$$

The upper limit for the i-th user's capacity under pre-equalization, corresponds to the ZF pre-equalizer. This is due to the channel flattening as a result of pre-equalization on each antenna, which transforms the frequency selective channel, on each antenna, into a narrowband frequency non-selective channel. The i-th user's capacity under ZF pre-equalization, denoted by $\mathbf{C}_{ZF}^{(i)}$, is given by:

$$
\begin{aligned}
\mathbf{C}_{ZF}^{(i)} &= \sum_{k \in \Psi_i} \log_2 \left(1 + \frac{E_s}{\mathbf{N}_T N_o} \mathbf{N}_T \sum_{j=1}^{\mathbf{N}_T} |\mathbf{P}_j|^2 \right) \\
&= \sum_{k \in \Psi_i} \log_2 \left(1 + \frac{E_s}{N_o} \sum_{j=1}^{\mathbf{N}_T} |\mathbf{P}_j|^2 \right)
\end{aligned} \tag{24}
$$

VI. RESULTS AND DISCUSSIONS

Table I shows the main simulation parameters used in this paper. We assume that the total number of sub-carriers N is 512 and that each user has access to 128 sub-carriers with a spreading factor Q of 4. For the 3GPP LTE standard the Spatial Channel Model (SCM) has been standardized to provide a so-called geometric or ray-based model [1]. The SCM defines three environments, namely i) Suburban Macro, ii) Urban Macro and iii) Urban Micro. Based on the 3GPP-SCM channel model, [15] presents a number of different channel models for indoor, rural urban and suburban microcells. Here, we assume the use of Urban LoS scenarios Range1 (LoS1 and LoS2) and Range2 B5b (LoS3) as well as Urban NLoS scenario C3 [15].

Carrier Frequency	2 GHz
Transmission Bandwidth	5 MHz
Total Number of Sub-carriers (N)	512
Number of Sub-carriers per User (M)	128
Guard Interval (P)	64
SC-FDMA Symbol Duration (μ)	150μs
Channel Knowledge	Perfect
Fading per tap	i.i.d. Rayleigh
Channel Coding	Not included
Signal Constellation	QPSK
Delay Profile	Model Dependent

TABLE I
SC-FDMA SIMULATION PARAMETERS

In this section we present the PAPR characteristics and the achievable capacity of the schemes discussed in sections III and IV. The results presented in this section were obtained using the channel models described in [15]. For each scenario, 10000 different channel realizations were simulated, where the phase of each tap was uniformly distributed in the interval $[0, 2\pi]$. All the results are then averaged over 10000 SC-FDMA symbols per user.

We assume that perfect knowledge of the channel state information (CSI) is available at the transmitter. Channel estimation is performed at the base-station, where the mean of the wideband channel is normalized to unity. The channel information is then sent back to the mobile unit. We ignore any overhead and latency issues.
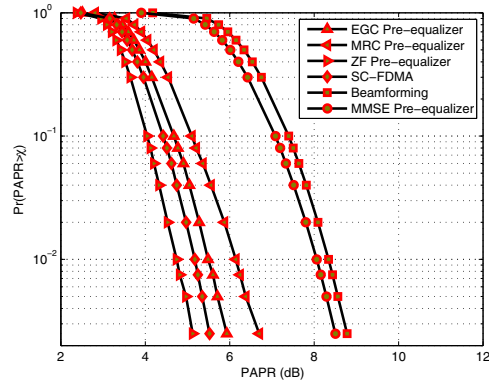

Fig. 2. PAPR per Antenna of Precoded and Pre-equalized MIMO SC-FDMA

Fig. 2 shows the Complementary Cumulative Distribution Function (CCDF) of the average PAPR per antenna for different precoded and pre-equalized two transmit antenna SC-FDMA systems for the NLoS channel scenario. As can be seen, the average PAPR varies with the utilized transmit processing technique. This is due to the different phases and gains on each of the sub-carriers as a result of precoding and pre-equalization, which increases the dynamic range of the precoded and pre-equalized waveforms. We also observe that the PAPR of the ZF pre-equalized waveform is lower than the PAPR of the non pre-equalized SC-FDMA waveform. In addition, although EGC pre-equalization increases the PAPR compared to the standard SC-FDMA waveform, this scheme offers a lower PAPR compared to MRC, MMSE and beam-forming. This is explained by the phase rotation introduced by EGC, which does not increase the dynamic range of the SC-FDMA waveform, but rather distorts the phases on all the sub-carriers. Furthermore, the average PAPR per antenna as a result of beamforming is is higher than the other pre-equalized SC-FDMA waveforms.

Fig. 3 shows the ergodic capacity per sub-carrier of the pre-equalizers presented in this work, for a SISO SC-FDMA system under a fading environment. We have only shown the ergodic capacity for scenarios LoS1 and NLoS. It was assumed that the multipaths for each channel realization for the channel fading case are complex independent and identically distributed (i.i.d) Rayleigh variables. These results show that the unconstrained ZF pre-equalizer achieves the Shannon AWGN capacity, which represents the upper bound of the achieved capacity for a single carrier system. In addition,
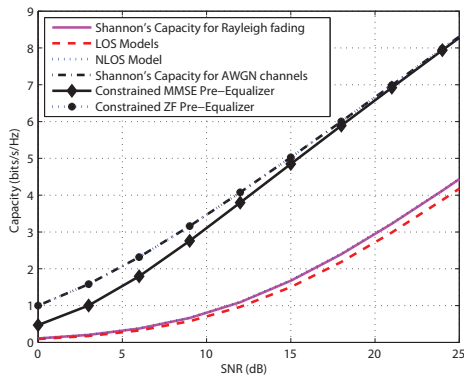
Fig. 3. Ergodic Channel Capacity of Pre-equalized SISO SC-FDMA for Faded Multipath Channel Scenarios

the unconstrained MMSE pre-equalizer converges towards the Shannon AWGN capacity for high SNR values. Furthermore, the achieved channel capacities of the constrained pre-equalizers is below Shannon's AWGN capacity curve, and equals the narrowband Rayleigh capacity. This is due to the power constraint applied to the pre-equalizers, which means that the pre-equalizer exploits the frequency selectivity of the channel but does not compensate for the fluctuations in the channel's mean power. In other words, pre-equalization is only concerned with flattening the channel and does not necessarily perform fast power control. For instance, in a narrowband channel constrained pre-equalization would play no role at the transmitter.
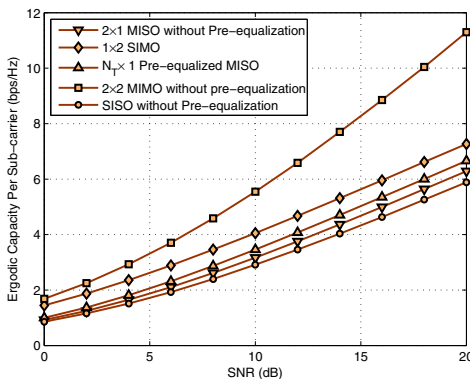

Fig. 4. Ergodic Channel Capacity of Pre-equalized MIMO SC-FDMA for Faded Multipath Channel Scenarios

Fig. 4 shows the ergodic capacity per sub-carrier for different MIMO SC-FDMA settings with and without constrained pre-equalization. As can be seen, the capacity of the standard pre-equalized MIMO SC-FDMA system increases by increasing both the number of transmit and receive antennas, which demonstrates how the spatial MIMO channel translates into an increase in the system throughput. As a result of pre-equalization, the capacity of the 2-by-1 increases compared to the the standard MIMO SC-FDMA. This capacity increase has a fixed capacity level that is irrespective of $\mathbf{N}_T$, as demonstrated in equation (24).

Fig. 5(a) and Fig. 5(b) show the BER performance of the
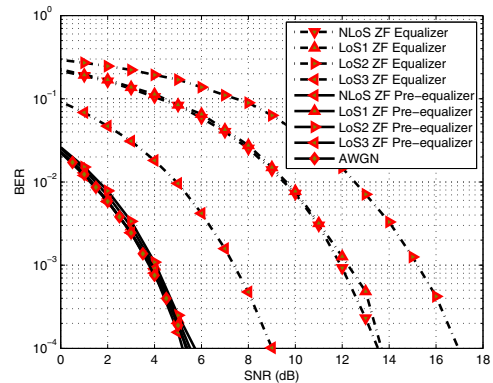
(a) BER Performance under ZF
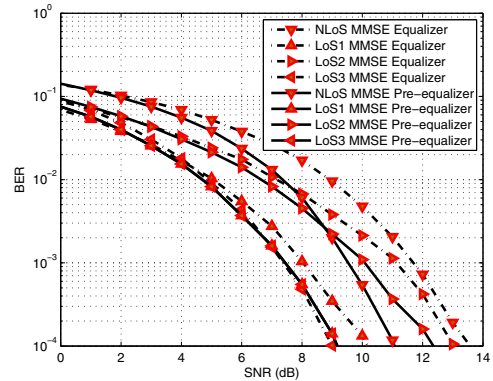
(b) BER Performance under MMSE

Fig. 5. BER Performance of the ZF and MMSE Equalizers and Pre-equalizers for SC-FDMA

ZF and MMSE equalizers and pre-equalizers, respectively for SISO SC-FDMA. The results are shown for a single resource unit occupying the first M sub-carriers and employing the L-FDMA sub-carrier mapping. We also assume perfect channel information at the transmitter. The results were obtained using the system parameters described in Table I. It was also assumed that the value of λ for the MMSE pre-equalizer was equal to N_o. Overall, the ZF based linear equalizer offers the worst BER performance compared to the other schemes for all channel scenarios. This is due to the noise enhancement resulting from the channel inversion applied by the ZF. The MMSE LE offers a performance that is superior to that of the ZF LE as it takes into account the presence of the noise at the receivers front-end. In contrast, the performance of the MMSE pre-equalizer compared to the MMSE equalizer depends on the channel delay profile. The ZF precoder offers a BER performance that is identical to the AWGN channel as a result of the channel inversion.

VII. CONCLUSION

In this paper we presented the use of frequency-domain precoding and pre-equalization for uplink MIMO SC-FDMA transmission. Overall, the ZF pre-equalizer offers the lowest PAPR compared to the other schemes. As a result of ZF pre-equalization, the transmission channel for each user is transformed into a flat frequency non-selective channel for

SISO SC-FDMA. The system therefore achieves a performance that is identical to the AWGN channel. For wideband Rayleigh fading channels, a single antenna single carrier system operating under the constrained ZF pre-equalizer is capable of achieving the capacity of the narrowband Rayleigh fading channel. However, if the transmit power of the system is not limited, in other words the pre-equalizer is not constrained, the system can achieve the capacity of an AWGN channel. This result can be used to exploit multi-user diversity when ZF pre-equalization is combined with a power and resource allocation scheme. In addition, for multiple transmit antenna systems, the use of pre-equalization also increases the system's capacity of MIMO SC-FDMA compared to the standard case. On the other hand, as the number of the transmit antennas increases, pre-equalization does not exploit the available MIMO spatial channel, as the overall capacity is equal to the case of two transmit antennas.

Although ZF pre-equalization achieves a superior BER performance compared to frequency domain equalization, there are two issues to be considered in the pre-equalizer design. Firstly, because the implementation of pre-equalization requires perfect knowledge of the uplink channel, with no latency, further work is required to address how channel estimation and tracking can assist the pre-equalizer in the case of mobility, channel estimation error and channel mismatch. Secondly, since the PAPR of the pre-equalizer's output is dependent on the channel fading, it is essential to employ PAPR reduction. Although PAPR reduction comes at the expense of performance degradation, the overall PAPR reduction must be greater than the loss in SNR for a given bit error rate.

REFERENCES

[1] 3GPP, "Technical Specification Group Radio Access Networks Physical layer aspects for evolved Universal Terrestrial Radio Access (UTRA)", 3GPP, Technical Specification TR 25.814 V7.1.0 Sep. 2006, Release 7

[2] R. van Nee, and R. Prasad, "OFDM for Wireless Multimedia Communications", Norwood, MA: Artech House, 2000.

[3] Hyung G. Myung, "Technical Overview of 3GPP Long Term Evolution (LTE)", http://hgmyung.googlepages.com/3gppLTE.pdf, Feb.8, 2007

[4] N. Tavangaran, A. Wilzeck, T. Kaiser, "MIMO SC-FDMA system performance for space time / frequency coding and spatial multiplexing", Smart Antennas, 2008. WSA 2008. International ITG Workshop on (2008), pp. 382-386.

[5] S. Jafar, S. Vishwanath and A. Goldsmith, "Channel capacity and beamforming for multiple transmit and receive antennas with covariance feedback"', ICC 01, 2001.

[6] A. Paulraj, R. Nabar and D. Gore, Introduction to Space-Time Wireless Communications, Cambridge University Press, Cambridge, UK, 2003.

[7] G. J. Foschini and M. J. Gans, "'On limits of wireless communications in a fading environment when using multiple antennas," Wireless Personal Communications, vol. 6, pp. 311-335, 1998.

[8] G.J. Foschini, "Layered space-time architecture for wireless communication in a fading environment when using multielement antennas," Bell Labs Tech. J., pp. 41-59, 1996.

[9] Hyung G. Myung, "Single Carrier Orthogonal Multiple Access Technique for Broadband Wireless Communication", Polytechnic University, January 2007

[10] Hyung G. Myung, Junsung Lim, and David J.Goodman, "Single Carrier FDMA for Uplink Wireless Transmission", 2006 IEEE Vehicular Technology Magazine 1 September 2006

[11] H. G. Myung, J.-L. Pan, R. Olesen, and D. Grieco, "Peak Power Characteristics of Single Carrier FDMA MIMO Precoding System", IEEE Vehicular Technology Conference (VTC) 2007 Fall, Baltimore, USA, Oct. 2007

[12] C. Ciochina, D. Castelain, D. Mottier and H. Sari, "A Novel Space-Frequency Coding Scheme for Single-Carrier Modulations," Proc. PIMRC 2007, September 2007, Athens, Greece.

[13] David Falconer, S. Lek Ariyavisitakul, Anader Benyamin-Seeyar, Brian Eidson, "Frequency Domain Equalization for Single-Carrier Broadband Wireless Systems", Communications Magazine, IEEE, Apr. 2002

[14] A. Goldsmith and P. Varaiya, "Capacity of fading channels with channel side information," Information Theory, IEEE Transactions on, vol. 43, no. 6, pp. 19861992, 1997.

[15] Final report on link level and system level channel Models, IST–2003–507581 WINNER D5.4 ver 1.4

[16] J. S. Hammerschmidt, C. Brunner, and C. Drewes, "Eigenbeamforming - A Novel Concept in Array Signal Processing," Proc. European Wireless Conference 2000, Dresden, Germany, Sep. 2000